Climatic Change (2023) 176:78
https://doi.org/10.1007/s10584-023-03548-7

Centenary (1930–2023) climate, and snow cover changes in the Western Alps of Italy. The Ossola valley

Leonardo Stucchi[1] · **Claudia Dresti**[2] · **Daniele Bocchiola**[1,3]

Received: 3 August 2022 / Accepted: 8 May 2023 / Published online: 12 June 2023

Abstract

In this paper, we study centennial trends of climate and snow cover within the Ossola valley, in the Western Italian Alps. We pursue different tests (Mann Kendall *MK*, bulk, and sequential/progressive *MKprog*, Linear Regression, also with change point detection, and moving window average *MW*) on two datasets, namely (i) *dataset1*, daily temperature, precipitation, snow depth for 9 stations in the area, during 1930–2018, and (ii) *dataset2*, snow depth and density, measured twice a month (from February 1st to June 1st) for 47 stations during 2007–2023. We also verify correlation with glacier retreat nearby. In *dataset1*, we highlight a positive trend for minimum temperature with MK, and Linear Regression. Using *MKprog*/MW, a negative change of snow cover depth, and duration starting from the late 1980s is found. In *dataset2*, despite the annual variability in snow cover and 2022–2023 winter drought, we assess the maximum snow water equivalent (SWE) to be delayed with respect to maximum snow depth at high altitude (over a month above 2.700 m a.s.l.), highlighting the effect of settling in decreasing snow depth during spring. We also present a formula linking through Linear Regression the Day of the Year of SWE peak to altitude, relevant to assess the onset of thaw season. Due to the high altitude of the stations, and the paradigmatic nature of the Ossola Valley, hosting Toce River, a main contributor to the Lake Maggiore of Italy, our results are of interest, and can be used as a benchmark for the Italian Alps.

Keywords Snow cover · Italian Alps · Snow density · Snow water equivalent · Climate time series · Climate change

✉ Leonardo Stucchi
leonardo.stucchi@polimi.it

Daniele Bocchiola
daniele.bocchiola@polimi.it

[1] Department of Civil and Environmental Engineering, Politecnico di Milano, L. da Vinci 32, 20133 Milan, Italy

[2] National Research Council, Water Research Institute, Largo Tonolli 50, 28922 Verbania Pallanza, Italy

[3] Associazione EVK2CNR, San Bernardino 145, 24126 Bergamo, Italy

1 Introduction

Mountain areas, especially the European Alps, are the most sensitive to climate change, displaying visible changes of landscape, and of cryosphere dynamics (e.g. Bocchiola and Diolaiuti 2010; Diolaiuti and Smiraglia 2010; Fugazza et al. 2021).

Glaciers shrinking and expansion phases are attributed to change in winter precipitation and summer temperature, where the latter plays a primary role as it affects not only snow and ice melt, but even flow velocity of glaciers (e.g. Mellor and Testa 1969; Duval et al. 1983). Because melting water percolates through the ice body until the bedrock, it reduces the friction, and the weight of ice (and snowpack) pushes the glacier with faster movement downstream.

Snow cover duration influences the hydrological cycle, as snowfields store water during winters, and release it during springs and summers (e.g. Confortola et al. 2013), therefore it has a great impact upon water availability for agriculture (e.g. Webb et al. 2021), hydropower production (e.g. Bombelli et al. 2019), river fauna (Palmer et al. 2009), and flora (Jonas et al. 2008). Furthermore, it has a direct economic value as it is crucial for winter mountain tourism and sport (Garavaglia et al. 2012).

For these reasons, it is clear why, even before widespread consciousness of anthropic influence on climate change, some scholars, among others Le Roy Ladurie (1971), tried to assess a “history of climate”, using no mathematical tools, but relying upon reports of the time about harvesting and trade. Climatic series were also reconstructed through quantitative analyses, especially in mountain areas, where proxies of ice core records, tree rings, sediment cores are relatively abundant. Such data allow to reconstruct temperature, and precipitation regime, even though with non-negligible uncertainty (Amrhein et al. 2020).

Continuous measurements of temperature and precipitation in mountain areas, which allowed to reconstruct consistent climates series, started during the eighteenth century in the European Alps, a most anthropized, and economically developed region worldwide, and they were collected and studied by several experts (e.g. Auer et al. 2007; Brugnara et al. 2012).

These records provide extraordinary documents, witnessing temperature increase in the last century, leading to a faster than ever glacier retreat, where Alps ice surface passed from (estimated) 4474 km^2 (Zemp et al. 2008) in 1850, to 1806 +/− 60 km^2 (−60%) in 2018 (Paul et al. 2020).

Despite the relative abundance of data regarding climate and glacier extension in the past, measured series of snow depth at high altitudes are quite rare, due to the intrinsic difficulty of measuring at stations in areas of extreme weather, and with no automatic instruments available until the mid 1990s in the Alps (Lehning et al. 1999). The building of dams for hydropower gave an impulse to continuous measurements of snow height and density, made possible, e.g. by the continuous presence of dam keepers, carrying among others the activity of evaluating stored water in the snowpack (snow water equivalent, SWE), and therefore potential hydropower production (e.g. Bocchiola and Diolaiuti 2010). Here, we exploit one such series of measured data, gathered in time by the personnel of the Italian National Electricity Board of Italy, Enel Green Power, acting within the high-altitude areas of the Ossola Valley, in the Western Italian Alps.

These high-altitude climatic data are used here to determine the effects of climate change on local alpine snow cover: particularly we investigate whether a reduction in snow can be related to changes in precipitation, temperature or both by applying a set of statistical analysis to evaluate trends, discontinuities and variations on series of temperature, precipitation and snow cover. We also assess variation with altitude and date in recent years (2007–2023) of snow depth and density. Being the study area part of the watershed of the Po River, watering a large lowland area for irrigation, drinking water, and hydropower (Bocchiola et al. 2013), our results can be used as a benchmark for other studies regarding the Alpine cryosphere, and for water-related assessment in the Po valley.

2 Materials and methods

2.1 Study area

Ossola is an alpine valley of the Piedmont region of Italy, covering most of the province of Verbano-Cusio-Ossola (Fig. 1). The province has an area of 2260 km^2, bordering at the East with Lombardy region and at the North with Swiss Cantons of Valais and Ticino. The valley is shaped by Toce River, springing from Riale Plan, in Formazza Valley (upper part of Ossola Valley), at 1800 m a.s.l., then running for 84 km, collecting water from minor side valleys, before the outlet at Maggiore Lake at 193.5 m a.s.l. The area is of great interest for water resources, given that Ossola Valley nests the Toce River (Ravazzani et al. 2016), a main contributor with Ticino River to the deep subalpine Lake Maggiore, the

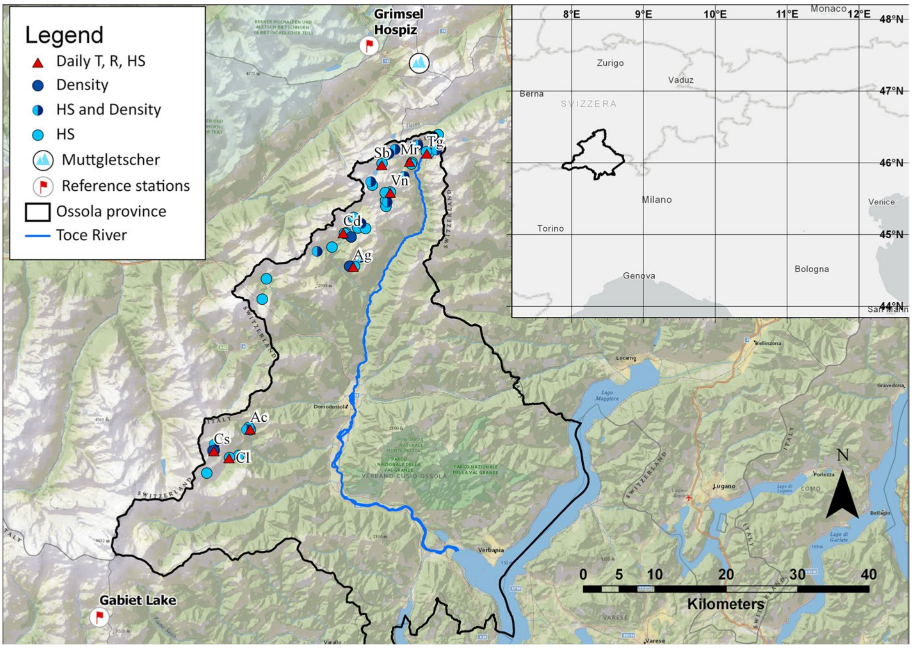

Fig. 1 Verbano-Cusio-Ossola study area. In red triangles daily stations from *dataset1*, in circles of different colors (according to the different measured variables) stations from *dataset2*, Toce river, considered reference stations and Muttgletscher. Reference System WGS84

second largest of Italy after Garda (212 km^2 vs 370 km^2). Thence, Ticino, as the outlet of Maggiore Lake, contributes to the Po River.

The region embeds some of the highest and majestic peaks of the Alps, the highest point being the Nordend peak (4609 m a.s.l.) of the Monte Rosa Massif, with an altitude range exceeding 4000 m a.s.l., and high variability in climate conditions. Climate is temperate at Lake Maggiore, with a yearly average air temperature of + 12.4 °C (min + 11.2 °C in 1956, max + 14.3 °C in 2003) during 1956–2006 at the station Verbania-Pallanza (211 m a.s.l.) (Ambrosetti et al. 2006) and extremely cold in Val Formazza, with yearly average temperature of 0.0 °C (+/− 6.7 °C) at Pian dei Camosci station at 2453 m a.s.l., with a humid temperate and subarctic climate, according to modified Koppen climate classification (Peel et al. 2007). Precipitation is relatively abundant in the Ossola province with 1680 mm on average yearly (estimated with Optimal Interpolation by Loglisci et al. 2012) vs. 1043 mm in the Piedmont region (estimate again with Optimal Interpolation, ARPA 2010).

Referring to the classification by Rau et al. (2005), of the many glaciers within the basin, only two are in the size class 2–5 km^2. Belvedere and Southern Ohsand have a measured area (in 2014) of 4.51 km^2, and 2.21 km^2 (Smiraglia and Diolaiuti 2016), and both are strongly retreating. Particularly, Ohsand Glacier is expected to largely shrink in the next 50 years, even with no large temperature increase hereon (Stucchi et al. 2019).

2.2 *Dataset1*

In the following sub-chapters, *dataset1* based on daily data is presented together with the applied test statistics and tools for the analysis.

2.2.1 Daily temperature, precipitation and snow depth data (1930–2018)

After the building of some dams for hydropower purposes in Ossola Valley, presently managed by ENEL Green Power company of Italy, weather stations were installed to monitor and forecast water inputs in the artificial lakes. Here, Enel Green Power made available daily records of maximum and minimum temperature $T_{max,min}$, Precipitation

Table 1 Daily measuring Stations with starting date (ending date is for all stations 31/12/2018) for each variable (T_{min} and T_{max}, minimum and maximum daily temperature in C°, *Rain* is liquid precipitation in mm (not available for Agaro station), *HS* is snow depth in cm) and coordinates in WGS84 UTM 32N

Name	ID			Starting date				Alt. [m a.s.l.]
		Lat	*Long.*	T_{min} [°C]	T_{max} [°C]	*P* [mm]	*HS* [cm]	
Toggia	Tg	46.44°	8.43°	01/01/1933	01/01/1935	01/11/1936	01/11/1936	2200
Morasco	Mr	46.43°	8.40°	01/01/1946	01/01/1946	01/01/1946	01/01/1946	1817
Sabbione	Sb	46.43°	8.35°	01/01/1951	01/01/1951	01/09/1953	01/01/1951	2462
Vannino	Vn	46.39°	8.37°	01/01/1930	01/01/1930	01/01/1951	01/11/1936	2180
Agaro	Ag	46.29°	8.30°	01/05/1950	01/05/1950	Na.	01/05/1950	1561
Codelago	Cd	46.34°	8.28°	01/01/1930	01/01/1930	01/01/1930	01/01/1930	1846
AlpeCavalli	Ac	46.09°	8.12°	01/01/1930	01/01/1930	01/01/1930	01/03/1931	1502
Camposecco	Cs	46.06°	8.05°	01/01/1934	01/01/1934	01/06/1937	01/01/1934	2330
Campliccioli	Cl	46.05°	8.08°	01/01/1930	01/01/1930	01/01/1930	01/11/1931	1356

P, and snow depth HS on the ground from 9 stations. Data availability ranges from 1930 to 2018, depending upon the site and variables (Table 1). The 3 stations of Alpe Cavalli, Camposecco and Campliccioli are located in the west of Domodossola, in Antrona Valley, whereas the other 6 are in the northern part, near the Swiss border, namely Codelago and Agaro in Antigorio Valley, and Morasco, Sabbione, Toggia, Vannino in Formazza Valley. The stations are all located at high altitudes between 1356 and 2462 m a.s.l., with a vertical jump of over 1100 m, and expected snow duration larger than half a year.

2.2.2 Temperature data quality assessment

Temperature data were measured with a maximum-minimum mercury thermometer that was reset everyday by the operator. Since no metadata are available, we do not know about the technical characteristics of the instruments, and of changes thereby. As a consequence, we cannot guarantee a priori the accuracy of the dataset (Aguilar et al. 2003), and correct maintenance of the stations, e.g. the absence of erroneous re-positioning that can bias the data (Böhm et al. 2010). We thus preliminarily proceed to verify the homogeneity, and dependability of the data. Internal coherence of the measurements is tested by evaluating the Pearson Correlation Coefficient τ_p of annual average T_{max} and T_{min} between the 9 stations. We obtain $\binom{9}{2} = \frac{(9)!}{(9-2)!(2)!} = 36$ values of correlation values between all the stations both for T_{max} and T_{min}, whose averages are equal to $\overline{\tau}_{p,Tmax}=0.27$, and $\overline{\tau}_{p,Tmin}$ 0.43. We also evaluate, as a term of comparison, τ_p for annual mean temperature from 48 stations located in Northern Italy of HISTALP dataset (already validated and used, to assess long-term temperature variations in the Alpine area, see Auer et al. 2007). Here, a much higher value is found $\overline{\tau}_{p,Thistalp}=0.82$. Given that the case study stations are located in a much smaller area with respect to HISTALP, and still the data are less correlated, we conclude that our temperature data (or part of them) are somewhat biased. Particularly $\tau_{p,av}$ is very low, because maximum temperature measurements, in case of (likely) misplacement of some thermometers, are generally more prone to errors, ca. the double of minimum (Böhm et al. 2010), as they can be affected by the sunlight. Furthermore, like reported by Aguado and Burt (2010), night-time temperature tends to be less variable with respect to daylight, and then minimum temperatures are representative of a larger number of hours. Thus, we neglect maximum temperature measurements in our analysis, and we consider minima only.

We then compare our data against those from the two nearest reference stations displaying continous measurements over the last century. One station is from HISTALP archives, namely Gabiet Lake (Fig. 1, ca. 25 km from nearest station), located in Valle D'Aosta region of Italy, where monthly homogenised mean temperature data are available during 1928–2006. The second one is the Grimsel Hospiz station in Bern Canton of Switzerland (Fig. 1, ca. 15 km from nearest station) where daily mean temperature is available since 1932 to the present days. We apply the Craddock test (Craddock 1979), which provides a visual assessment of the degree of homogeneity of candidate series, by assessing the cumulative difference between the reference, and the tested series, corrected with a monthly delta to ensure that the mean values of the two series are equal (and the extremes of the series equal to 0). In Fig. 2, we report the output of the test for the two reference stations, highlighting the two series with the smallest discrepancy with respect to the reference series, i.e. Campliccioli and Alpe Cavalli. Because a potential inhomogeneity is detected in

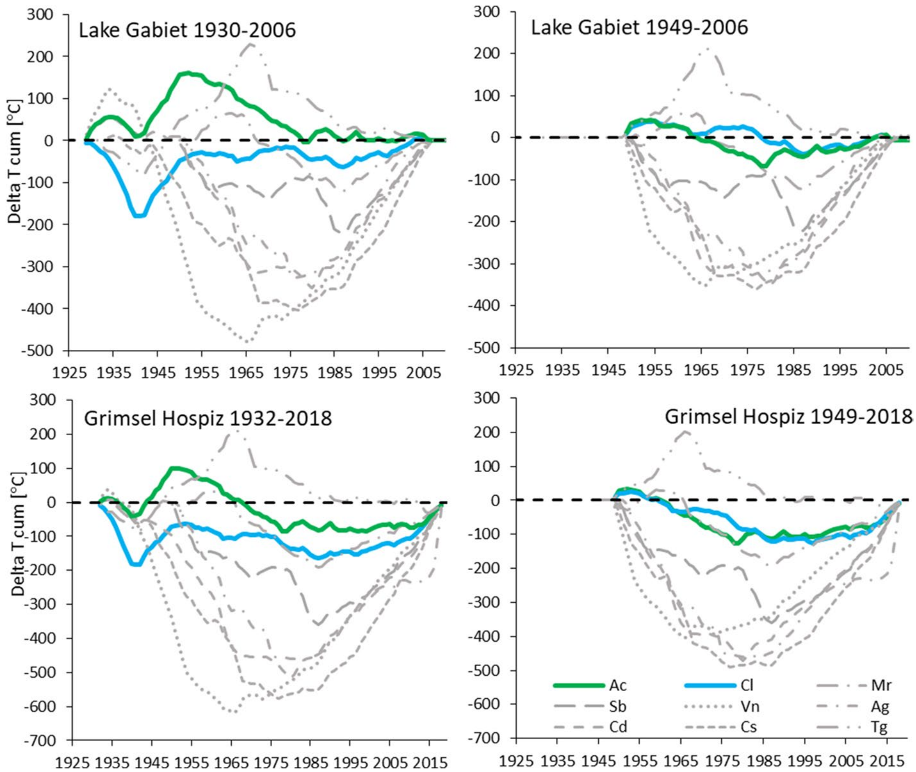

Fig. 2 Craddock test of temperature data using as reference stations Lake Gabiet, for the whole period (**a**) and optimal (**b**), and Grimsel Hospiz for the whole period (**c**), and optimal (**d**). Highlighted in blue and green the two recording stations with best performance

the first years of measurements, we neglect measurements before 1949, so largely increasing the correspondence between candidate series and reference ones. Accordingly, test statistics for temperature are applied only to these two stations.

2.2.3 Precipitation correction using fresh snowfall

As well as air temperature, also total precipitation P (mm) is difficult to measure in the high mountains, because of (strong) wind, and low accuracy in the assessment of snow water content by (heated) rain gauges (Kochendorfer et al. 2022), with local studies pointing to an underestimation of snow water content down to −70% (Mazza and Mercalli 1992). Thus, we consider not reliable the readings of the gauges in the presence of snow and we clean precipitation series by considering null the measurements whenever maximum daily temperature is below 0 °C. In this way, we extract a series of daily rainfall R only, unless for the mixed precipitation events, generally occurring with air temperature near 0°, which here are confused with rain events. Finally, we assess solid precipitation S, i.e. snow contribute, deducing fresh snowfall HN (cm) from the (positive) variations of snow depth (e.g. Bocchiola and Rosso 2007) as follows:

$$\begin{aligned} HN_d &= HS_d - HS_{d-1} \ if \ HS_d > HS_{d-1} \\ HN_d &= 0 \ if \ HS_d \le HS_{d-1} \\ S_d &= \frac{\rho_n}{\rho_w}[\cdot] \cdot HN_d[cm] \cdot 10[mm \cdot cm^{-1}] \end{aligned} \tag{1}$$

where suffix d is for a given day, ρ_w is [kg/m^3] water density and ρ_n is fresh snow density. We use here an average value valid for the Italian Alps, $\rho_n = 115$ kg/m^3 (Valt et al. 2018). After computing liquid and solid precipitation, we can assess total precipitation P (mm) as follows:

$$P_d[mm] = R_d[mm] + S_d[mm] \tag{2}$$

Once computed precipitation, we also add up as testing variable P_{days}, e.g. the number of days with precipitation larger than 1 mm.

2.2.4 Snow-related variables

In order to examine the seasonality of snow cycle, we consider other additional derived variables, i.e. (i) snow cover duration *D0*, or number of days in the hydrologic year (September–August), when snow depth is above 0 cm), (ii) snow cover start, and end, SC_{start} and SC_{end}, i.e. the first and last day when snow is present on the ground, (iii) maximum and average snow depth, HS_{max} and HS_{av} [cm], and (iv) average fresh snow, *HN* [cm]. The variables are also considered at seasonal scale, therefore in Winter (December to February), Spring (March to April), Summer (June to August) and Fall (September to November).

2.2.5 Test statistics

In addition to Long-Term Mean and related standard deviation, to evaluate potential presence of trends for each variable, we use the following tests (see e.g. Bocchiola 2014).

1) Linear Regression, with significance given using p-value, with a level α=5%. This test allows to highlight (significant) linear trends, which are also pursued using a Change-Point detection procedure, below.

2) Moving Window average *MW* (De Michele et al. 1998). The moving average is taken over a period of 30 years, as suggested, e.g. by WMO (2017), and then compared with long-term average *LT*. If *MW* is not contained within the *LT* confidence interval with α=5% the hypothesis of stationarity of the data can be rejected.

3) Mann Kendall *MK* (Kendall 1975), also in the progressive version (MK_{prog}, used to detect the starting point of a trend). This is a non-parametric test, i.e. it does not take into account any hypothesis about the type (linear/non-linear) of trend, and it is therefore a complement to Linear Regression analysis.

4) Change-Point analysis, including an abrupt change of the mean, *MCP*, and of slope, *LRCP*, using Matlab package *findchangepts* (Killick et al. 2012). This method, frequently used in hydrology (e.g. Wang et al. 2014, Valentin et al. 2018), is based on the hypothesis

$$H_0 : \tau_1 = \tau_2 = \cdots = \tau_n = \tau_{(1)} \tag{3}$$

$$H_1 : \tau_{(1)} = \tau_1 = \tau_2 = \cdots = \tau_k \ne \tau_{k+1} = \cdots = \tau_n = \tau_{(2)}. \tag{4}$$

Therein, $\tau_{(1)}$ and $\tau_{(2)}$ are the statistical properties of interest (here, mean value, and slope) of a first and a second part of the dataset. Given the probability density function of x^* observation $P(X^*)$, the maximum log-likelihood of the alternate hypothesis H_1 is

$$\log P\left(x^*_{1:k}|\tau^*_{(1)}\right) + \log P\left(x^*_{1:k}|\tau^*_{(2)}\right), \tag{5}$$

where $\tau^*_{(1)}$ and $\tau^*_{(2)}$ are the maximum likelihood estimates of the statistical properties. After locating the change-point k, if the ratio between H_1 and H_0 is above a predetermined threshold, the change of τ is accepted. Furthermore, to avoid a change-point to be detected in response to (few) anomalous values at the two ends of the series, we decide to neglect the change-points located within 10 years from the start/end of the measurements. Then, an *F*-Test is pursued, with α = 5%, for the two periods identified by *MCP*, to verify the presence of a change in the variance of the data, at the change of magnitude point.

2.2.6 Correlation analysis and ice depletion

All the variables analysed here are compared through correlation matrices using the Pearson coefficient τ_p, to establish a possible correlation/causality with retreat of glaciers nearby. We use for the purpose the measured annual (outlet length) variation at the front of *Muttgletscher* (Fig. 1), a small ice body (0.36 km^2 in 2018) located in the Swiss Canton of Valais, at ca. 10 km from the nearest analysed station, the changes of which are registered since 1918 (GLAMOS 2022). The main Italian glaciers in the area, Belvedere and Hosand, are not suitable for this analysis, due both to short/sparse data series (of outlet length), and to their larger size, likely implying a slower response in time of the glaciers (e.g. Bahr et al. 1998; Marta et al. 2021), which makes yearly glacier changes less reactive to local variation in climate (temperature, etc.). Other nearer glaciers (e.g. Corno Glacier, Griessgletscher, Gornergletscher) on the Swiss side were also considered, but due to their larger size and/or lack of snout data therein, they display no meaningful correlation with our dataset.

2.3 *Dataset2*

As done for *dataset1*, here we illustrate *dataset2* and inherent test statistics.

2.3.1 Snow depth and density data 2007–2023

In addition to the daily series, Enel Green Power also provided data of snow depth (43 stations) and density (17 stations), measured manually with snow core samplers (Fig. 1, SM Table 1). The measurements are performed twice a month during February 1st to June 1st, i.e. 9 times per year, during 2007–2023. In the 15 stations where we have both snow depth, and density data, we can also evaluate Snow Water Equivalent, i.e. SWE (mm) on the ground as

$$SWE[mm] = HS[cm] \bullet \frac{\rho_{sw}}{\rho_w}[\cdot] \bullet 10[\frac{mm}{cm}] \tag{6}$$

where ρ_{sw} [kg/m^3] is the measured snow (pack) density.

2.3.2 Mean and altitudinal gradient

Simple average values of snow depth, snow density and SWE are evaluated for each date during 2007–2023. Due to scarce length of the series, Linear Regression vs time is not recommended here (WMO 2017), but we still pursue a Linear Regression vs altitude to assess change of the considered variables thereby. Particularly, in order to assess end of accumulation period, i.e. start of thawing, we consider through Linear Regression the delay with respect to altitude of the Day of the Year when peak of SWE is reached. Namely, we assess for each station the average through 2007–2023 of the sequential day number of the year (starting day 1 on September 1st as we consider it as the start of a hydrological year) when assessed SWE is maximum, and then we perform Linear Regression of these day numbers vs. the altitude of the stations. We repeat the same procedure also for HS to verify the correspondence in time of the peak of HS and SWE at different altitude values.

3 Results

3.1 Long-term analysis

We report here in summary Tables 2, 3, 4, 5, 6, and 7 the outcomes of the calculated statistics. For each statistic, unless for Long-Term Mean, we highlight only significant results ($a = 5\%$) as previously reported in Sect. 2.2.5. Due to (bad) quality assessment, as explained, we consider only the values of T_{min} from Alpe Cavalli and Camplìccioli, while we neglect the other ones (still reported in italics). Outputs of the *MK*, and *MW* tests are given as 1/0, i.e. when non-stationarity is accepted/rejected.

In Tables 2, 3, 4, 5, 6, and 7, one can notice how different variables are differently responsive to the considered tests. For instance, HS_{av} and HS_{max} display significant changes according to the Linear Regression, *MCP* and *MK* tests, while no significant response is found for the *MW*, whereas other variables (e.g. *S0*) change visibly according to the latter test. As a graphical support to Tables 6 and 7, we also report in Fig. 3 the absolute frequency distribution of the years when a change is detected (with *MCP*, and MK_{prog}) for main snow variables (i.e. HS_{av}, HS_{max}, *D0*).

Table 2 Outputs for Linear Regression (bold if significant) for the variables T_{min} (only Camplìccioli and Alpe Cavalli reported as significant) *P*, *R* (*Not Available* for Agaro stations), P_{days} HS_{av}, HS_{max}, *HN*, *S0*, *E0*, *D0*

ID	T_{min}	*P*	*R*	P_{days}	HS_{av}	HS_{max}	*HN*	*S0*	*E0*	*D0*
		Linear Regression Coefficient [/year]								
Tg	*−0.006*	*−0.8*	*−1.1*	0.11	**−0.5**	**−1.4**	*0.1*	**−0.22**	*0.12*	*0.00*
Mr	*0.016*	**5.1**	**5.9**	0.10	**−0.5**	**−1.4**	*−0.6*	*−0.04*	*−0.19*	**−0.44**
Sb	*0.044*	*2.3*	**3.5**	0.13	**−0.5**	**−1.1**	*−1.8*	*−0.12*	*−0.18*	*−0.19*
Vn	*0.036*	*−1.6*	**−3.3**	**0.23**	**−0.5**	**−1.4**	*−1.4*	*−0.19*	*0.01*	*0.08*
Ag	*0.067*	*Na.*	*Na.*	*Na.*	**−0.2**	**−1.0**	*−1.2*	*0.20*	*0.15*	**−0.49**
Cd	*0.031*	*−2.8*	*−2.2*	−0.08	*−0.1*	*−0.5*	*−0.5*	*−0.02*	*0.04*	*0.02*
Ac	**0.014**	*−1.2*	*−1.1*	−0.07	*−0.1*	*−0.4*	*−0.5*	*−0.06*	*−0.01*	*−0.18*
Cs	*0.048*	**−4.8**	**−4.9**	−0.03	**−0.6**	**−1.6**	*−1.8*	*0.05*	**−0.18**	*−0.26*
Cl	**0.013**	*2.7*	*2.3*	0.10	**−0.2**	*−0.5*	*−0.2*	*0.04*	*−0.04*	**−0.24**

Table 3 Outputs for Long-Term Mean for the variables T_{min} (only Camplicciolі and Alpe Cavalli reported as significant) *P*, *R* (*Not Available* for Agaro stations), P_{days} HS_{av}, HS_{max}, *HN*, *S0*, *E0*, *D0*

	T_{min}	P	R	P_{days}	HS_{av}	HS_{max}	HN	$S0$	$E0$	$D0$
	Long-Term Mean ± Standard Deviation									
To	*− 2.9 ± 1.0*	**1704 ± 318**	**901 ± 225**	**113 ± 14**	**98 ± 37**	**307 ± 89**	**698 ± 165**	**31.3 ± 18.2**	**298.4 ± 32.9**	**235.9 ± 26.0**
Mr	*0.4 ± 0.9*	**1697 ± 327**	**1087 ± 280**	**108 ± 13**	**61 ± 28**	**226 ± 77**	**530 ± 153**	**47.7 ± 19.0**	**268.8 ± 25.2**	**197.9 ± 27.4**
Sb	*− 4.1 ± 1,3*	**1551 ± 307**	**706 ± 255**	**109 ± 17**	**124 ± 14**	**347 ± 82**	**734 ± 158**	**21.4 ± 15.6**	**329.9 ± 25.7**	**261.9 ± 20.1**
Vn	*− 3.6 ± 1.7*	**1797 ± 401**	**1081 ± 325**	**108 ± 19**	**96 ± 39**	**301 ± 100**	**622 ± 239**	**36.4 ± 20.9**	**295.7 ± 30.8**	**230.5 ± 27.6**
Ag	*1.8 ± 2.0*	*Na.*	*Na.*	*Na.*	**31 ± 17**	**157 ± 60**	**394 ± 130**	**60.2 ± 19.0**	**252.5 ± 19.6**	**162.5 ± 27.8**
Cd	*− 0.9 ± 1.3*	**1973 ± 421**	**1330 ± 311**	**115 ± 14**	**74 ± 30**	**256 ± 82**	**559 ± 165**	**46.6 ± 17.0**	**281.0 ± 18.8**	**212.0 ± 21.8**
Ac	**2.5 ± 0.8**	**1788 ± 432**	**1376** ±340	**101 ± 13**	**25 ± 18**	**139 ± 66**	**358 ± 164**	**63.1 ± 20.9**	**247.9 ± 15.0**	**152.6 ± 33.1**
Cs	*− 2.4 ± 1.5*	**1775 ± 435**	**981 ± 348**	**102 ± 15**	**80 ± 43**	**278 ± 130**	**690 ± 210**	**34.8 ± 18.8**	**295.0 ± 19.4**	**235.6 ± 21.3**
Cl	**3.6 ± 0.7**	**1831 ± 459**	**1461 ± 357**	**98 ± 14**	**24 ± 17**	**138 ± 75**	**322 ± 158**	**66.9 ± 20.5**	**244.4 ± 13.8**	**154.1 ± 28.3**
Mean	*− 0.6 ± 1.2*	**1618 ± 361**	**991 ± 305**	**99 ± 15**	**68 ± 30**	**239 ± 85**	**545 ± 171**	**45.4 ± 18.9**	**279.3 ± 22.4**	**204.8 ± 26.0**

Table 4 Outputs for Moving Window Average (1 if unstationarity is detected) for the variables T_{min} (only Camplicciolі and Alpe Cavalli reported as significant) *P*, *R* (*Not Available* for Agaro stations), P_{days} HS_{av}, HS_{max}, *HN*, *S0*, *E0*, *D0*

	T_{min}	P	R	P_{days}	HS_{av}	HS_{max}	HN	$S0$	$E0$	$D0$
	Moving Window Average									
To	*0*	**1**	**0**	**0**	**0**	**0**	**0**	**0**	**0**	**0**
Mr	*0*	**0**	**0**	**1**	**0**	**0**	**1**	**1**	**0**	**0**
Sb	*0*	**1**	**0**	**1**	**1**	**1**	**1**	**1**	**1**	**0**
Vn	*0*	**0**	**0**	**0**	**0**	**0**	**0**	**0**	**0**	**0**
Ag	*0*	*Na.*	*Na.*	*Na.*	**0**	**0**	**1**	**1**	**0**	**0**
Cd	*0*	**1**	**1**	**0**	**1**	**0**	**1**	**1**	**0**	**0**
Ac	**0**	**1**	**1**	**0**	**0**	**0**	**1**	**1**	**0**	**0**
Cs	*0*	**0**	**0**	**0**	**0**	**0**	**1**	**1**	**0**	**0**
Cl	**0**	**1**	**1**	**1**	**0**	**1**	**1**	**1**	**0**	**0**

Figure 3 clearly shows that, in 15 cases out of the 32, when changes in one variable are detected, these changes happen in the second half of the 1980s (with one peak in 1987, 9 occurrences). We also show in Fig. 4 the mean annual values of snow depth HS_{av} in our 9 stations. Given the visibly large variability of HS_{av}, a specific year (or a short time window) when abrupt changes happen, they cannot be detected. Local minima can be seen in 1988 that would explain the 3 changing points in 1987 for *MCP*.

Table 5 Outputs for *Mann Kendall p*-value (bold if trend is detected) for the variables T_{min} (only Campliccioli and Alpe Cavalli reported as significant) *P*, *R* (*Not Available* for Agaro stations), P_{days} HS_{av}, HS_{max}, *HN*, *S0*, *E0*, *D0*

	T_{min} Mann Kendall *p* value	*P*	*R*	P_{days}	HS_{av}	HS_{max}	*HN*	*S0*	*E0*	*D0*
To	*0.29*	*0.65*	*0.14*	*0.19*	**0.01**	**< 0.01**	*0.89*	**0.01**	*0.70*	*0.29*
Mr	*0.00*	**< 0.01**	**< 0.01**	*0.16*	**< 0.01**	**< 0.01**	*0.53*	*0.55*	**0.02**	**< 0.01**
Sb	*0.00*	*0.22*	**0.03**	*0.66*	**0.04**	*0.06*	**0.03**	*0.30*	*0.30*	*0.08*
Vn	*0.00*	*0.19*	**0.01**	**0.04**	**0.01**	**< 0.01**	**0.04**	*0.05*	*0.60*	*0.78*
Ag	**< 0.01**	*Na.*	*Na.*	*Na.*	**0.03**	**< 0.01**	*0.12*	*0.23*	*0.45*	**0.01**
Cd	*0.00*	*0.06*	**0.03**	*0.23*	*0.41*	*0.26*	*0.43*	*0.87*	*0.63*	*0.79*
Ac	*0.45*	*0.42*	*0.23*	*0.21*	*0.06*	*0.11*	*0.42*	*0.95*	*0.71*	*0.15*
Cs	*0.00*	**0.01**	**< 0.01**	*0.33*	**< 0.01**	**< 0.01**	*0.12*	*0.51*	**0.02**	**< 0.01**
Cl	**< 0.01**	*0.1*	*0.1*	*0.10*	**0.01**	*0.07*	*0.58*	*0.53*	*0.17*	**0.01**

Table 6 Outputs for *Mann Kendall progressive* for the variables T_{min} (only Campliccioli and Alpe Cavalli reported as significant) *P*, *R* (*Not Available* for Agaro stations), P_{days} HS_{av}, HS_{max}, *HN*, *S0*, *E0*, *D0*

	T_{min} Mann Kendall progressive	*P*	*R*	P_{days}	HS_{av}	HS_{max}	*HN*	*S0*	*E0*	*D0*
Tg					**1967**			**1963**		
Mr			**1980**		**1984**	**1987**				**1988**
Sb	*1996*		**1987**							
Vn	*1985*	**1969**								
Ag	*1977*	*Na.*	*Na.*	*Na.*		**1991**	**1987**			
Cd	*1993*									
Ac					**1988**					**1992**
Cs	*1986*	**1972**	**1961**		**1978**	**1987**				**1995**
Cl	**2008**				**1987**					**1988**

3.2 Correlation analysis

In Fig. 5, we show a correlation matrix developed for some of the most significantly correlated variables. The highest correlation is found between snow duration *D0*, average snow depth HS_{av}, and seasonal cumulated fresh snow *HN*. Particularly, we find that spring and fall snowfall affects *D0* more than winter snowfall, while HS_{av} is affected largely by fall and winter snowfall, possibly remaining on the ground even after spring. Rainfall amount is weakly related against other variables, except for a significant correlation between its value in spring, and fall, i.e. with a delay of one season.

Seasonal temperatures are also correlated to each other, but they have apparently weak impact upon snow variables. However, significant correlation of temperature is found against changes of the *Muttgletscher* front, especially for spring temperature (T_{spr}, −0.30). Also, slight correlation is seen against the new snow amount in the year HN_{spr}, clearly pointing at an indication of the nourishing/shielding effect of snow for glaciers (e.g. Diolaiuti et al. 2012a, b).

Table 7 Outputs for *Linear Regression Change Point*, *Mean Change Point* and the related two mean values for the variables T_{min} (only Campliccioli and Alpe Cavalli reported as significant) *P*, *R* (*Not Available* for Agaro stations), P_{days} HS_{av}, HS_{max}, *HN*, *S0*, *E0*, *D0*

	T_{min}	*P*	*R*	P_{days}	HS_{av}	HS_{max}	*HN*	*S0*	*E0*	*D0*
	Linear Regression change point									
Mr		**2002**	**2002**							
Mean change point										
Tg					**1964**	**1964**		**1961**		
Mr		**1977**	**1980**		**1987**	**1988**				**1987**
Sb			**1991**		**1987**	**2004**	**1987**			**2002**
Vn				**1934**	**1964**	**1964**	**1964**			
Ag		*Na.*	*Na.*	*Na.*	**1987**	**1988**	**1987**			**1987**
Cd						**1988**				
Ac				**1942**	**1981**	**1981**				
Cs		**1979**	**1962**		**1979**		**1987**		**2003**	**1986**
Cl	**2008**				**1981**					**1987**
Mean 1°/2° period										
Tg					**115/87**	**353/278**		**40/26**		
Mr		**1,569/ 1,811**	**942/ 1,214**		**71/47**	**256/186**				**209/183**
Sb			**658/824**		**134/112**	**360/299**	**781/678**			**266/248**
Vn				**74/112**	**114/83**	**362/264**	**748/628**			
Ag		*Na.*	*Na.*	*Na.*	**36/26**	**179/130**	**437/343**			**175/148**
Cd						**271/228**				
Ac				**109/99**	**29/19**	**152/120**				
Cs		**1,897/ 1,620**	**1,237/ 911**		**96/62**		**228/153**		**298/281**	**242/226**
Cl	**3.4/4.4**				**29/18**					**161/142**

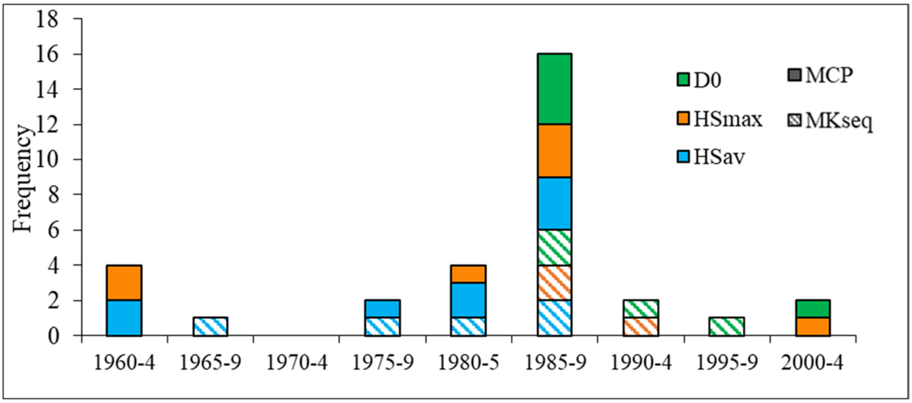

Fig. 3 Absolute frequency of changing year (with p value < 0.05), for the variables HS_{av}, HS_{max} and $D0$ for the test MK_{prog} and MCP

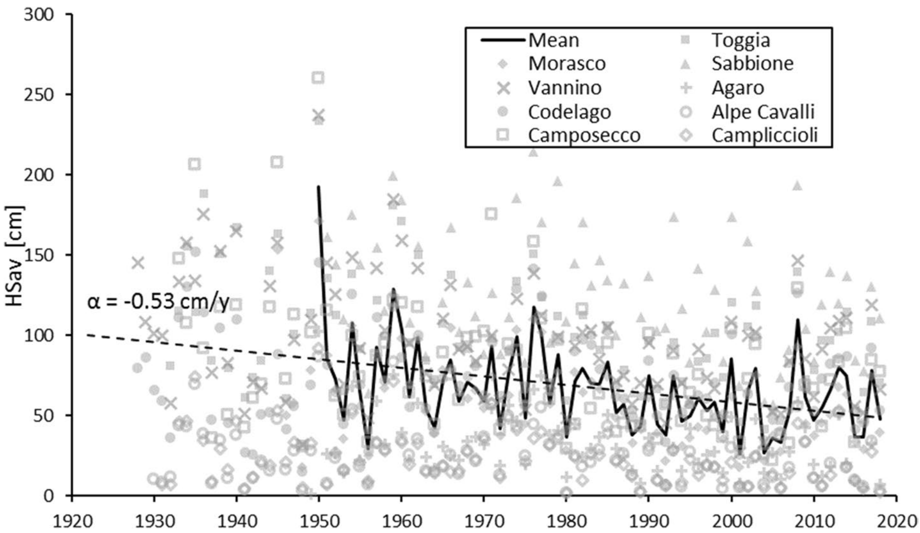

Fig. 4 Annual Mean Snow Depth (HS_{av}) from daily data of 9 stations (in grey). It is also reported the average between the stations (black) and linear trend (dotted black) with coefficient α

3.3 Snow depth and density 2007–2023

In Fig. 6, we report the mean values of SWE assessed for *dataset2* (2007–2023). We notice a quite high interannual variability with 2009 as year with the highest snow cover (+74% with respect to the 2007–2023 average), and 2022 and 2023 (last measurement available on April 1st) as the driest years (−70% and −69% with respect to 2007–2023 average).

In Table 8, we report mean, Linear Regression coefficient against altitude, and determination coefficient R^2, for *HS*, snow on ground density, and the variable SWE assessed. In addition to the mean values, we also report in Fig. 7 the confidence limits as given

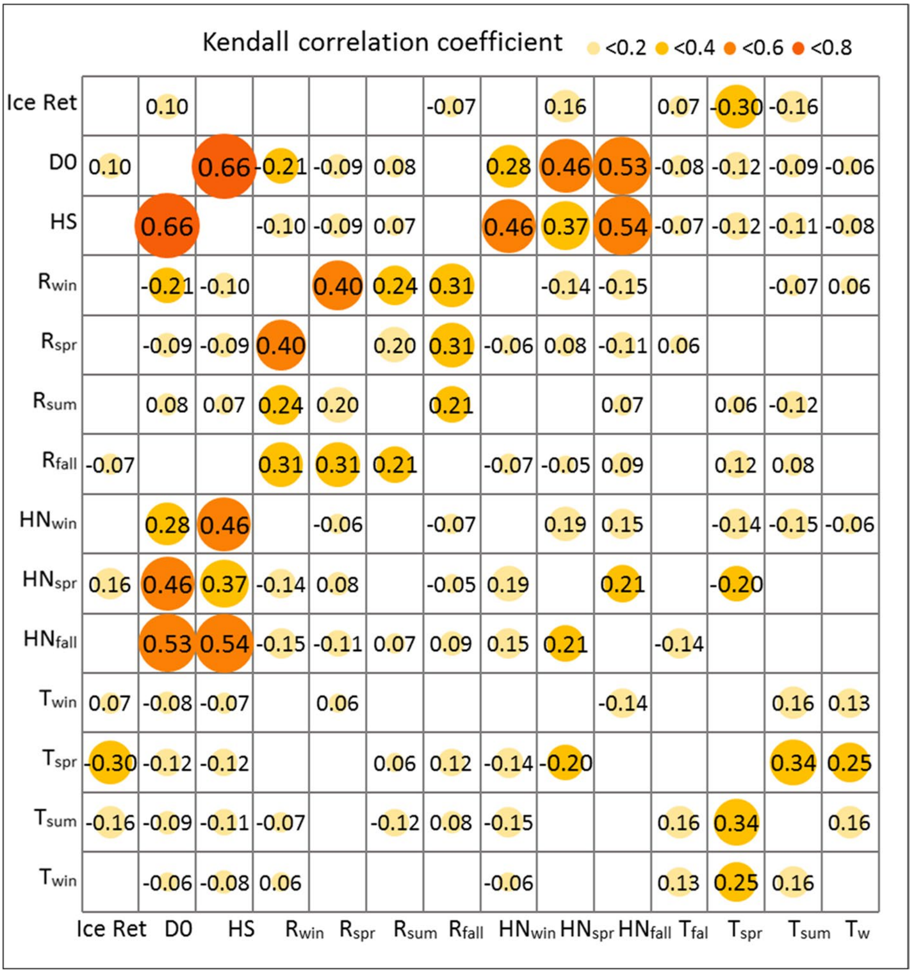

Fig. 5 Correlation Matrix for annual (*Ice Ret.*, *D0*, *HS*) and seasonal variables. *T* is average annual minimum temperature, *Ice Ret.* is front variation of *Muttgletscher* (+advance, −retreat). Size of circles and colors refer to absolute value of Kendall (light yellow if $|\rho|<0.2$, yellow if $0.2<|\rho|<0.4$, light orange if $0.4<|\rho|<0.6$, orange if $0.6<|\rho|<0.8$). Not significant coefficients (p-value>0.05) are not reported

by standard deviation, and the mean altitude of the measuring stations for each day and variable. *HS* reaches a mild peak on April 1[st], followed by slow decrease, becoming rapider after May. On the other hand, SWE displays a flatter curve with higher variability during spring, as also noticeable from Fig. 6. The regression coefficients here show increasing values of *HS* and SWE for higher altitudes. Mean snow density increases from winter to spring, clearly due to snow settling (e.g. Bocchiola and Diolaiuti 2010). However, there is a seemingly little lapse rate against altitude, if not for a quick decrease in May–June. This is likely the result of snow accumulation, larger at higher altitudes and thereby continuing even after spring onset, and snow freeze–thaw cycle, more intense at the lowest altitudes.

Finally, in Fig. 8 we report a (linear) relationship between altitude, the date of maximum snow depth (HS_{max}) (a), and the date of maximum *SWE*, i.e. the end date of the

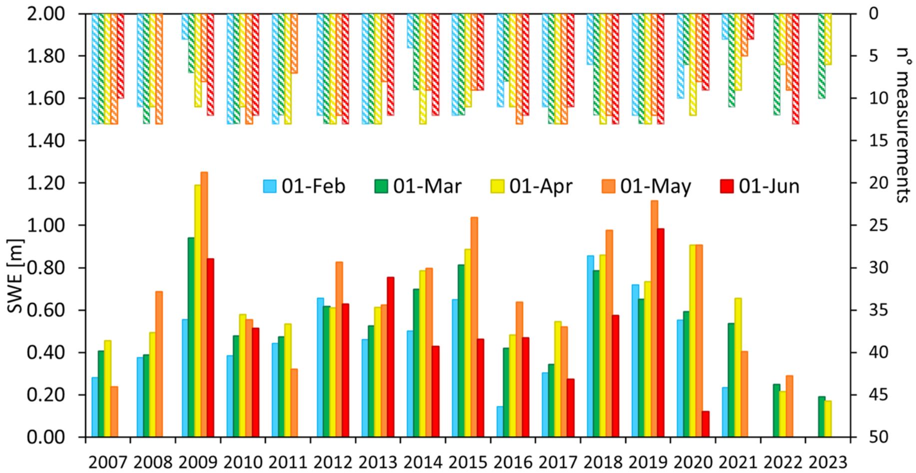

Fig. 6 Time series of average SWE for the 1st of February, March, April, May and June. On the secondary y axis number of measuring stations are reported

accumulation period of snow (b). Particularly, on the *y* axis, we provide the average Day of the Year (among the sampled ones) when HS/SWE reaches annual peak (HS_{max}, SWE_{max}), against the altitude of the station in the *x* axis. We also report a Linear Regression slope β thereby, which displays a delay of peak every 100 m of altitude jump equal to 4.8 for *HS* and + 7.3 for *SWE*, with significant determination coefficient R^2. The two regression lines cross on February 25th at 1580 m a.s.l., meaning that above that altitude, we assess SWE peak to be delayed of 2.5 days every 100 m with respect to HS peak.

4 Discussion

In this section, we compare our results with available literature, highlighting potential implications of interest.

4.1 Long-term data — dataset1

4.1.1 Precipitation

Total precipitation, and accordingly number of days with precipitation, does not seem to follow a visible trend according to our Linear Regression test. This result, which could also be due to an approximation in our assessment (i.e. considering constant snow density), is in agreement with several studies for Alpine areas. Among others, Brunetti et al. (2006) analysed long-term precipitation stations in Italy including the ones from the above-mentioned HISTALP dataset, and they found no significant decrease for NW of Italy where *dataset1* stations are located. Also, Brugnara and Maugeri (2019) found, in Rosmini Domodossola station in Ossola Valley, only a weak decrease (ca. −5%) of total precipitation in the last 150 years. Even extending the analysis to the sixteenth century, Casty et al. (2005) were

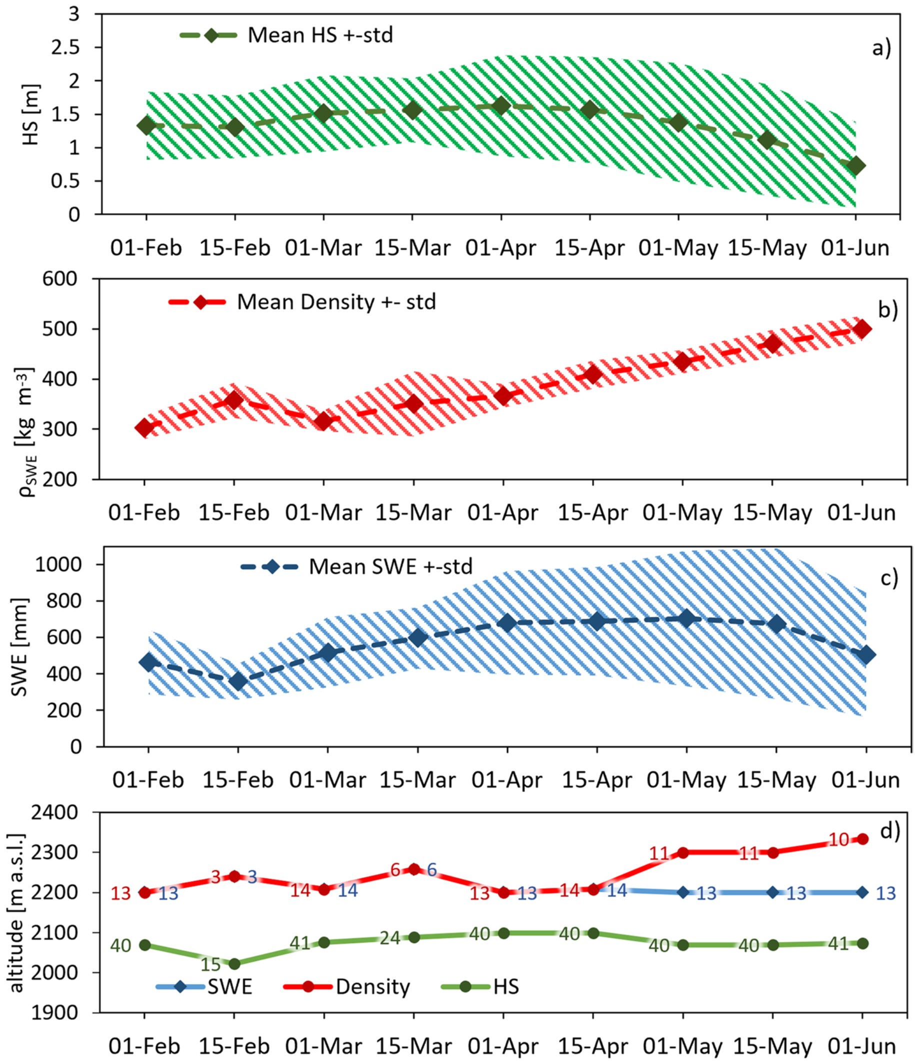

Fig. 7 Mean *HS* (**a**), snow pack density (**b**), *SWE* (**c**) and confidence level (+/−1 standard deviation) for the period 2007–2023. In subplot (**d**) it is also reported the altitude of the measuring stations and the number of measurements (in text) for each variable

not able to detect a widespread long-term trend, but rather few local anomalies, like we observed here for 5 stations with the *MW* test. The high interannual variability of precipitation is a main cause of difficult trend detection that also was found to be variable both in space and time in the Alpine area, and again not significant for SW area embedding Ossola Valley (Auer et al. 2007). Even correlation analysis against annual temperature changes, or against global climate indices, such as the North Atlantic Oscillation NAO, gave poor results hitherto (e.g. Schmidli et al. 2002; Bocchiola and Diolaiuti 2010). Moreover, when a nexus between NAO and precipitation was detected, it showed to be unstable, with large changes through time, especially after the 1980s (Colombo et al. 2022).

Table 8 Mean values and altitudinal gradient, Linear Regression, and related determination coefficient R^2 of snow depth *HS* (43 stations, average altitude 2.074 m a.s.l.), snow density (17 stations, average altitude 2.250 m a.s.l.), and snow water equivalent (*SWE*) (14 stations, average altitude 2.213 m a.s.l.) for *dataset*2 (2007–2023)

	HS			Snow density [kg m^3]			SWE [mm]		
Date	Mean [cm]	Linear Regression [cm·km^{-1}]	R^2	Mean [kg m^3]	Linear Regression [kg m^3 km^{-1}]	R^2	Mean [mm]	Linear Regression [mm·km^{-1}]	R^2
01-Feb	120	+95	0.47	303	27	0.01	464	+1162	0.52
15-Feb	112	+76	0.32	358	59	0.01	358	−2406	0.88
01-Mar	148	+107	0.47	317	34	0.03	518	+934	0.43
15-Mar	125	+131	0.67	351	−26	0.04	597	+42	0.00
01-Apr	169	+160	0.51	366	−13	0.06	680	+755	0.57
15-Apr	161	+178	0.57	409	−18	0.01	690	+645	0.49
01-May	136	+199	0.68	435	−47	0.01	704	+586	0.58
15-May	96	+195	0.75	470	−201	0.00	675	+559	0.66
01-Jun	67	+143	0.65	500	−150	0.26	504	+662	0.63

4.1.2 Snow depth and duration

While yearly mean snow HS_{av} is the result of an interaction between snowfall, compaction and melting throughout the whole year (e.g. Sommerfeld and LaChapelle 1970), HS_{max} is mostly affected by phenomena occurring in the accumulation period, i.e. between (late) October and spring. As such, both variables are frequently used to study cryospheric trends (e.g. Dyrrdal et al. 2013; Marty and Blanchet 2012). As we showed in Tables 2, 3, 4, 5, 6, 7, we find relevant reduction of both variables, either as a trend (Linear Regression, and *MK*) or as a discontinuity (*MKPROG*, *MCP*). In Fig. 3, we also display how most of the changing points here are located in the late 1980s. Indeed, this result seems confirmed by some previous works in the Alpine area. Marty (2008) studied the number of snow days in the Swiss Alps, in 34 stations, and found an abrupt drop after 1988–1989, but with no specific trend, as verified both with *MK* and Linear Regression. In the Adige valley (NE Italian Alps), Marcolini et al. (2017) observed significantly lower snow depth in 1988–1999 with respect to 1980–1987.

Snow cover duration *D0* is also quite responsive to climate change (Tables 2, 3, 4, 5, 6, and 7 and Fig. 3) and similarly to *HS* for several stations changing point is located in the 1980s. Nevertheless, Linear Regression is reliable only for 3 stations below 2000 m a.s.l. and provides a maximum reduction of ca. −5 days for decade, and still lower than values assessed by Klein et al. (2016) for the Swiss Alps (average −8.2 days for decade). This inequality worth to be more thoroughly explored, could also be due to the quite different time window considered (from 1930s–1950s to 2018 here vs. 1975–2015 in the Klein study).

4.1.3 Temperature

Linear Trend analysis provides significant results for Camplicciolí station, where an increase of +0.016 °C year^{-1} during 1949–2018 is detected. This value is slightly lower,

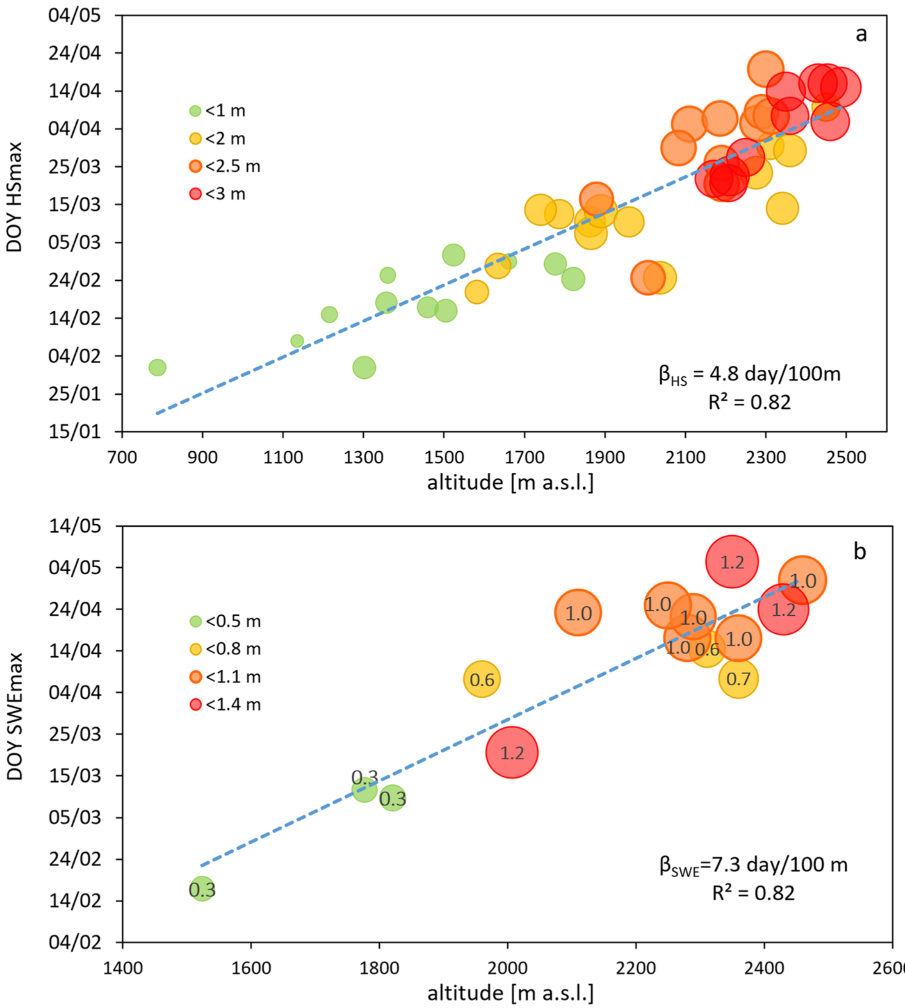

Fig. 8 Linear Regression between average Day of the Year of peak of *HS* [m] (**a**) and *SWE* [m] (**b**) and respective station altitude. The average HS_{max} and value is represented by the circle size and color and for SWE_{max} it is also reported in the label

but still consistent with respect to + 0.023 °C year^{-1} during 1950–2000 as reported by Auer et al. (2007) in SW Alps. We also found a break point for temperature in recent years, in 2008 (mean + 3.4 °C in 1949–2007 vs + 4.4 °C in 2008–2018). Such noticeable jump is coherent with global data, witnessing a temperature increase of + 0.240 °C during the 2000s to 2010s (GISTEMP 2022).

4.1.4 Correlation among variables

Negative, weak correlation was found between temperature and springtime/autumn snowfall, while no correlation was found in winter, when at the high altitude of our stations, the effect of warming is still less visible (i.e. temperature remains mostly below 0 °C), as reported, e.g. by Serquet et al. for the Swiss Alps (2011). No significant correlation was found between total precipitation and temperature, with only a small correlation between summer temperature and precipitation, coherently with results from Brunetti et al. (2009) where a similar negative coefficient was found for the SW alpine area, nesting the Piedmont region.

The nexus between glacier retreat and temperature increase is well known and established in literature (Haeberli and Beniston 1998), but the correlation between the two variables at yearly scale cannot always be given for granted. In addition to (winter) precipitation, other phenomena can lead the relationship between glacier retreat and temperature (very) far from linearity. Glaciers' inertia, redistribution of snow by avalanche and wind, debris covering, plus change in ice dynamics, as occurred in the Belvedere Glacier nearby (Haeberli et al. 2002) largely impact annual ice front variation. To partially mitigate these effects, Kendall correlation is considered instead of Pearson, which reduces the impact of eventual outliers due to one of the aforementioned phenomena. Despite limitations in the methodology, *Muttgletscher* variations are here coherent/correlated with spring and summer temperature, and (less) with seasonal snowfall *HN*, whereas correlation between (solid) precipitation and ice loss, is well assessed in literature, albeit generally lower than the correlation between the latter and temperature (e.g. Colucci and Guglielmin 2015). Lack of correlation here is most probably due to a larger variability of precipitation with respect to temperature, meaning that values of precipitation assessed in a study area could be less representative of *Muttgletscher* area, on the Northern side of the Alps. In fact, using the HISTALP dataset we assess correlation between average yearly temperature between NW and SW Alpine region, where *Muttgletscher* and the study area are located respectively, and we find $\tau_p = 0.93$, while on the other side correlation coefficient for annual precipitation for the same regions is much lower $\tau_p = 0.32$.

4.2 Density and snow water equivalent — *dataset2*

Maximum snow depth values measured on April 1st from *dataset2* are coherently lower with respect to *dataset1* (169 vs 239 cm) since this variable has shown to be quite responsive to climate change (Table 2, picture 3). Because in *dataset2*, the measurements of snow depth end before total ablation, no conclusions concerning snow cover duration between the two datasets can be set forth.

Schöber et al. (2016) analysed the long-term mean (1952–2010) of snow depth, and density for the Tyrolean Alp, at stations between 1400 and 2000 m a.s.l. (vs 1500–2500 m a.s.l. here), and found lower values of snow depth, 0.9 m at April 1st (vs 1.69 m here), but more similar values of density, with 350 kg m^{-3} at April 1st (vs 366 kg m^{-3} here), and 400 kg m^{-3} at May 1st (vs 435 kg m^{-3} here). While snow density is knowingly conservative (e.g. Bocchiola 2010), higher snow depth values point towards a likely different temperature, and winter precipitation regimes.

Despite the limitation given by the coarse temporal resolution of the dataset and the swinging between wet (e.g. 2009) and dry years (e.g. 2022, 2023), we also notice a lag, increasing with altitude, between maximum snow depth, and maximum SWE, which we assess to be over a month above 2700 m a.s.l. Knowingly in the present literature thaw period is conventionally cast at April 1st (e.g. Ranzi et al. 1999; Bohr and Aguado 2001), but its dependence upon elevation here depicted was also claimed before (e.g. Bocchiola and Groppelli 2010). The lag of thaw period at high altitude may be likely explained by considerable snowfall contribution even during some springs, maybe camouflaged in terms of snow depth by settling. Another explaining factor can be the refreezing of spring rainfall that then becomes part of the snowpack. This phenomenon was observed, e.g. by Gugerli et al. (2019). They studied a snowfield above Plaine Morte Swiss glacier, at 2690 m a.s.l., and found a similar delay with the peak of SWE in late May, while the measured *HS* was already on a downward trend since April. A correct assessment of SWE_{max} and of the related date/period can be crucial to predict melt/stream flows in a dry spring/summer, especially in high altitude catchments (Jenicek et al. 2018), whereas better performance in hydrological modeling may be achieved considering spring rainfall as (potential) new SWE when snow cover is present. The relationship here displayed between SWE_{max} date, and altitude seems relevant in this sense.

5 Conclusions

In this paper, we analyse two high altitude datasets covering Ossola Valley, in the Piedmont region of Italy, namely (i) *dataset1*, a long-term daily dataset (1930–2018) with measurements of snow depth, precipitation, and temperature, and (ii) *dataset2,* with more recent (2007–2023) periodic (at fixed dates) data of snow depth and density. The *dataset1* dataset, due to the expected evolution in time of measuring tools, and possibly changes in site and setting of the stations, passed through a data quality assessment by correlation analysis and Craddock test. We could highlight changes of behavior of *dataset1* data in the second half of the 1980s, when sensibly thinner snow cover than before is detected. Snow depth and density measurements in *dataset2* allow us to define an equation linking the date of the annual peak of snow depth and SWE with respect to altitude, with which we also detect a shift between SWE peak and snow depth peak, increasing with altitude. The results we report are of interest as a benchmark in the area, and deserve further investigation, also to assess potential effects thereby upon hydrological cycle in Alpine streams for water resources management under climate change.

Supplementary Information The online version contains supplementary material available at https://doi.org/10.1007/s10584-023-03548-7.

Acknowledgements Personnel of the National Electric Power Agency of Italy ENEL Green Power is kindly acknowledged for providing their data for the study. The study is in fulfilment of the activity of Climate-Lab of Politecnico di Milano, www.climatelab-polimi.it, under the umbrella of the Memorandum of Understanding between Politecnico di Milano-DICA Dept., and CNR-IRSA, for "Joint cooperation in the field of water resources management, and the effects of climate change in the high altitude areas".

Author contribution Stucchi Leonardo (corresponding author): Conceptualization, Methodology, Formal analysis, Writing.

Dresti Claudia: Data curation, Writing, Project administration.

Bocchiola Daniele: Methodology, Writing, Project administration.

Funding Open access funding provided by Politecnico di Milano within the CRUI-CARE Agreement.

Data Availability Data will be available upon reasonal request from the corresponding author.

References

Aguado E, Burt JE (2010) Understanding weather & climate, 3rd edn. Pearson Education, Upper Saddle River, New Jersey, p 560

Aguilar E, Auer I, Brunet M, Peterson TC, Wieringa J (2003) Guidance on metadata and homogenization. Wmo Td 1186(January 2003):1–53

Ambrosetti W, Barbanti L, Rolla A (2006) The climate of Lago Maggiore area during the last fifty years. J Limnol 65(1):1–62. https://doi.org/10.4081/jlimnol.2006.s1.1

Amrhein DE, Hakim GJ, Parsons LA (2020) Quantifying structural uncertainty in paleoclimate data assimilation with an application to the last millennium. Geophys Res Lett 47(22):e2020GL090485. https://doi.org/10.1029/2020GL090485

ARPA Piemonte [Regional Environment Protection Agency of Piedmont] (2010) Trends of precipitation. Available in Italian at: http://rsaonline.arpa.piemonte.it/meteoclima50/tendenza_precipitazioni.htm

Auer I, Böhm R, Jurkovic A, Lipa W, Orlik A, Potzmann R, Schöner W, Ungersböck M, Matulla C, Briffa K, Jones P, Efthymiadis D, Brunetti M, Nanni T, Maugeri M, Mercalli L, Mestre O, Moisselin JM, Begert M, Müller-Westermeier G, Kveton V, Bochnicek O, Stastny P, Lapin M, Szalai S, Szentimrey T, Cegnar T, Dolinar M, Gajic-Capka M, Zaninovic K, Majstorovic Z, Nieplova E (2007) HISTALP—historical instrumental climatological surface time series of the Greater Alpine Region. Int J Climatol: J R Meteorol Soc 27(1):17–46. https://doi.org/10.1002/joc.1377

Bahr DB, Pfeffer WT, Sassolas C, Meier MF (1998) Response time of glaciers as a function of size and mass balance: 1. Theory. J Geophys Res: Solid Earth 103(B5):9777–9782

Bocchiola D (2010) Regional estimation of snow water equivalent in the Italian Alps using kriging. Geogr Fis Dinam Quat 33:3–14 (**10 figg., 3 tabb**)

Bocchiola D (2014) Long term (1921–2011) hydrological regime of Alpine catchments in Northern Italy. Adv Water Resour 70:51–64. https://doi.org/10.1016/j.advwatres.2014.04.017

Bocchiola D, Groppelli B (2010) Spatial estimation of Snow Water Equivalent at different dates within the Adamello Park of Italy. Cold Reg Sci Technol 63(3):97–109. https://doi.org/10.1016/j.coldregions.2010.06.001

Bocchiola D, Rosso R (2007) The distribution of daily snow water equivalent in the central Italian Alps. Adv Water Resour 30(1):135–147

Bocchiola D, Diolaiuti G (2010) Evidence of climate change within the Adamello Glacier of Italy. Theoret Appl Climatol 100:351–369. https://doi.org/10.1007/s00704-009-0186-x

Bocchiola D, Nana E, Soncini A (2013) Impact of climate change scenarios on crop yield and water footprint of maize in the Po valley of Italy. Agric Water Manag 116:50–61. https://doi.org/10.1016/j.agwat.2012.10.009

Böhm R, Jones PD, Hiebl J, Frank D, Brunetti M, Maugeri M (2010) The early instrumental warm-bias: a solution for long central European temperature series 1760–2007. Clim Change 101(1):41–67. https://doi.org/10.1007/s10584-009-9649-4

Bohr GS, Aguado E (2001) Use of April 1 SWE measurements as estimates of peak seasonal snowpack and total cold-season precipitation. Water Resour Res 37(1):51–60. https://doi.org/10.1029/2000WR900256

Bombelli GM, Soncini A, Bianchi A, Bocchiola D (2019) Potentially modified hydropower production under climate change in the Italian Alps. Hydrol Process 33(17):2355–2372. https://doi.org/10.1002/hyp.13473

Brugnara Y, Maugeri M (2019) Daily precipitation variability in the southern Alps since the late 19th century. Int J Climatol 39:3492–3504. https://doi.org/10.1002/joc.6034

Brugnara Y, Brunetti M, Maugeri M, Nanni T, Simolo C (2012) High-resolution analysis of daily precipitation trends in the central Alps over the last century. Int J Climatol 32(9):1406–1422

Brunetti M, Maugeri M, Monti F, Nanni T (2006) Temperature and precipitation variability in Italy in the last two centuries from homogenised instrumental time series. Int J Climatol: J R Meteorol Soc 26(3):345–381. https://doi.org/10.1002/joc.1251

Brunetti M, Lentini G, Maugeri M, Nanni T, Auer I, Boehm R, Schoener W (2009) Climate variability and change in the Greater Alpine Region over the last two centuries based on multi-variable analysis. Int J Climatol: J R Meteorol Soc 29(15):2197–2225. https://doi.org/10.1002/joc.1857

Casty C, Wanner H, Luterbacher J, Esper J, Böhm R (2005) Temperature and precipitation variability in the European Alps since 1500. Int J Climatol: J R Meteorol Soc 25(14):1855–1880. https://doi.org/10.1002/joc.1216

Cat Berro D, Mercalli L, Bertolotto PL, Mosello R, Rogora M, Orrù A (2014) Il clima dell'Ossola Superiore. Nimbus 72:46–129

Colombo et al (2022) Long-term trend of snow water equivalent in the Italian Alps. J Hydrol. https://doi.org/10.1016/j.jhydrol.2022.128532

Colucci RR, Guglielmin M (2015) Precipitation–temperature changes and evolution of a small glacier in the southeastern European Alps during the last 90 years. Int J Climatol 35(10):2783–2797. https://doi.org/10.1002/joc.4172

Confortola G, Soncini A, Bocchiola D (2013) Climate change will affect hydrological regimes in the Alps. A case study in Italy. Rev Geogr Alp (101–3). https://doi.org/10.4000/rga.2176

Craddock JM (1979) Methods for comparing annual rainfall records for climatic purpose. Weather 34:332–346

De Michele C, Montanari A, Rosso R (1998) The effect of non-stationarity on the evaluation of critical design storms. Water Sci Tech 37(11):187–193. https://doi.org/10.2166/wst.1998.0465

Diolaiuti GA, Bocchiola D, Vagliasindi M, D'agata C, Smiraglia C (2012a) The 1975–2005 glacier changes in Aosta Valley (Italy) and the relations with climate evolution. Prog Phys Geogr 36(6):764–785. https://doi.org/10.1177/0309133312456413

Diolaiuti G, Bocchiola D, D'agata C, Smiraglia C (2012b) Evidence of climate change impact upon glaciers' recession within the Italian Alps. Theor Appl Climatol 109(3):429–445. https://doi.org/10.1007/s00704-012-0589-y

Diolaiuti G, Smiraglia C (2010) Changing glaciers in a changing climate: how vanishing geomorphosites have been driving deep changes in mountain landscapes and environments. Géomorphol: relief processus environ 16(2):131–152. https://doi.org/10.4000/geomorphologie.7882

Duval P, Ashby MF, Anderman I (1983) Rate-controlling processes in the creep of polycrystalline ice. J Phys Chem 87(21):4066–4074. https://doi.org/10.1021/j100244a014

Dyrrdal AV, Saloranta T, Skaugen T, Stranden HB (2013) Changes in snow depth in Norway during the period 1961–2010. Hydrol Res 44(1):169–179. https://doi.org/10.2166/nh.2012.064

Fugazza D, Manara V, Senese A, Diolaiuti G, Maugeri M (2021) Snow cover variability in the greater alpine region in the MODIS era (2000–2019). Remote Sens 13(15):2945. https://doi.org/10.3390/rs13152945

Garavaglia V, Diolaiuti G, Smiraglia C et al (2012) Evaluating tourist perception of environmental changes as a contribution to managing natural resources in glacierized areas: a case study of the Forni Glacier (Stelvio National Park, Italian Alps). Environ Manage 50:1125–1138. https://doi.org/10.1007/s00267-012-9948-9

Giaccone E, Colombo N, Acquaotta F, Paro L, Fratianni S (2015) Climate variations in a high altitude Alpine basin and their effects on a glacial environment (Italian Western Alps). Atmósfera 28(2):117–128

GLAMOS (2022) Swiss Glacier Length Change, release 2022. Glacier Monitoring Switzerland. https://doi.org/10.18750/lengthchange.2022.r2022

Gugerli R, Salzmann N, Huss M, Desilets D (2019) Continuous and autonomous snow water equivalent measurements by a cosmic ray sensor on an alpine glacier. Cryosphere 13(12):3413–3434. https://doi.org/10.5194/tc-13-3413-2019

Haeberli W, Beniston M (1998) Climate change and its impacts on glaciers and permafrost in the Alps. Ambio 258–265. https://www.jstor.org/stable/4314732

Haeberli W, Kääb A, Paul F, Chiarle M, Mortara G, Mazza A, Deline P, Richardson S (2002) A surge-type movement at Ghiacciaio del Belvedere and a developing slope instability in the east face of Monte Rosa, Macugnaga, Italian Alps. Norweg J Geogr 56:104–111

Jenicek M, Seibert J, Staudinger M (2018) Modeling of future changes in seasonal snowpack and impacts on summer low flows in alpine catchments. Water Resour Res 54:538–556. https://doi.org/10.1002/2017WR021648

Jonas T, Rixen C, Sturm M, Stoeckli V (2008) How alpine plant growth is linked to snow cover and climate variability. J Geophys Res Biogeosci 113(G3). https://doi.org/10.1029/2007JG000680

Kendall MG (1975) Rank correlation methods. Oxford Univ Press, New York

Killick R, Fearnhead P, Eckley IA (2012) Optimal detection of changepoints with a linear computational cost. J Am Stat Assoc 107(500):1590–1598. https://doi.org/10.1080/01621459.2012.737745

Klein G, Vitasse Y, Rixen C, Marty C, Rebetez M (2016) Shorter snow cover duration since 1970 in the Swiss Alps due to earlier snowmelt more than to later snow onset. Clim Change 139:637–649. https://doi.org/10.1007/s10584-016-1806-y

Kochendorfer J, Earle M, Rasmussen R, Smith C, Yang D, Morin S, Mekis E, Buisan S, Roulet YA, Landolt S, Wolff M, Hoover J, Thériault JM, Lee G, Baker B, Nitu R, Lanza L, Colli M, Meyers T (2022) How Well Are We Measuring Snow Post-SPICE? Bull Amer Meteor Soc 103:E370–E388. https://doi.org/10.1175/BAMS-D-20-0228.1

Lehning M, Bartelt P, Brown B, Russi T, Stöckli U, Zimmerli M (1999) SNOWPACK model calculations for avalanche warning based upon a new network of weather and snow stations. Cold Reg Sci Technol 30(1–3):145–157. https://doi.org/10.1016/S0165-232X(99)00022-1

Le Roy Ladurie E (1971) Times of feast, times of famine. Doubleday, Garden City, NY

Loglisci N, Rivella E, Tomassone L, Garnero G, Godone G (2012) Il clima. Clima e biodiversità. Esperienze di monitoraggio in ambiente alpino [The climate. Climate and biodiversity. [Experiences of monitoring in Alpine environment]. Rivella E., Converso C. & Nappi P. (a cura di). Tipografia Bolongaro snc, Baveno, VB

Maisch M (2000) The long-term signal of climate change in the Swiss Alps: Glacier retreat since the end of the Little Ice Age and future ice decay scenarios. Geogr Fis Din Quat 23(2):139–151

Marcolini G, Bellin A, Disse M, Chiogna G (2017) Variability in snow depth time series in the Adige catchment. J Hydrol: Reg Stud 13:240–254. https://doi.org/10.1016/j.ejrh.2017.08.007

Marta S, Azzoni RS., Fugazza D, Tielidze L, Chand P, Sieron K, ..., Ficetola GF (2021) The retreat of mountain glaciers since the Little Ice Age: a spatially explicit database. Data 6(10):107. https://doi.org/10.3390/data6100107

Marty C (2008) Regime shift of snow days in Switzerland. Geophys Res Lett 35(12). https://doi.org/10.1029/2008GL033998

Marty C, Blanchet J (2012) Long-term changes in annual maximum snow depth and snowfall in Switzerland based on extreme value statistics. Clim Change 111(3):705–721. https://doi.org/10.2166/nh.2012.064

Maugeri M (2009) Climate variability and change in the Greater Alpine Region over the last two centuries based on multi-variable. Int J Climatol 29:2197–2225. https://doi.org/10.1002/joc.1857

Mazza A, Mercalli L (1992) Il Ghiacciaio Meridionale dell'Hohsand (Alta Val Formazza): un secolo di evoluzione climatica ei rapporti con la produzione idroelettrica. Oscellana 22(1):30–44

Mellor M, Testa R (1969) Effect of temperature on the creep of ice. J Glaciol 8(52):131–145. https://doi.org/10.3189/S0022143000020803

GISTEMP Team, 2023: GISS Surface Temperature Analysis (GISTEMP), version 4. NASA Goddard Institute for Space Studies. https://data.giss.nasa.gov/gistemp/. Accessed 23 Dec 2022

Palmer MA, Lettenmaier DP, Poff NL, Postel SL, Richter B, Warner R (2009) Climate change and river ecosystems: protection and adaptation options. Environ Manage 44(6):1053–1068. https://doi.org/10.1007/s00267-009-9329-1

Paul F, Rastner P, Azzoni RS, Diolaiuti G, Fugazza D, Le Bris R, Nemec J, Rabatel A, Ramusovic M, Schwaizer G, Smiraglia C (2020) Glacier shrinkage in the Alps continues unabated as revealed by a new glacier inventory from Sentinel-2. Earth Syst Sci Data 12:1805–1821. https://doi.org/10.5194/essd-12-1805-2020

Peel MC, Finlayson BL, McMahon TA (2007) Updated world map of the Köppen-Geiger climate classification. Hydrol Earth Syst Sci 11(5):1633–1644. https://doi.org/10.5194/hess-11-1633-2007

Rahel FJ, Olden JD (2008) Assessing the effects of climate change on aquatic invasive species. Conserv Biol 22(3):521–533. https://doi.org/10.1111/j.1523-1739.2008.00950.x

Ranzi R, Grossi G, Bacchi B (1999) Ten years of monitoring areal snowpack in the Southern Alps using NOAA-AVHRR imagery, ground measurements and hydrological data. Hydrol Process 13:2079–2095. https://doi.org/10.1002/(SICI)1099-1085(199909)13:12/13%3c2079::AID-HYP875%3e3.0.CO;2-U

Rau F, Mauz F, Vogt S, Khalsa SJS, Raup B (2005) Illustrated GLIMS glacier classification manual. Inst Physische Geographie Freiburg Germany National Snow Ice Data Cent Boulder USA Vers 1:755. https://doi.org/10.1016/j.rse.2005.07.004

Ravazzani G, Dalla Valle F, Gaudard L, Mendlik T, Gobiet A, Mancini M (2016) Assessing climate impacts on hydropower production: the case of the Toce River Basin. Climate 4(2):16. https://doi.org/10.3390/cli4020016

Schmidli J, Schmutz C, Frei C, Wanner H, Schär C (2002) Mesoscale precipitation variability in the region of the European Alps during the 20th century. Int J Climatol: J R Meteorol Soc 22(9):1049–1074. https://doi.org/10.1002/joc.769

Schöber J, Achleitner S, Bellinger J, Kirnbauer R, Schöberl F (2016) Analysis and modelling of snow bulk density in the Tyrolean Alps. Hydrol Res 47(2):419–441. https://doi.org/10.2166/nh.2015.132

Serquet G, Marty C, Dulex J-P, Rebetez M (2011) Seasonal trends and temperature dependence of the snowfall/precipitation-day ratio in Switzerland. Geophys Res Lett 38:L07703. https://doi.org/10.1029/2011GL046976

Smiraglia C, Diolaiuti GA (2016) Lo stato attuale dei ghiacciai italiani e la loro recente evoluzione. Ist Lombardo-Accad Sci Lett-Rend Sci. https://doi.org/10.4081/scie.2016.539

Sommerfeld RA, LaChapelle E (1970) The classification of snow metamorphism. J Glaciol 9(55):3–18

Stucchi L, Bombelli GM, Bianchi A, Bocchiola D (2019) Hydropower from the Alpine cryosphere in the era of climate change: the case of the Sabbione Storage Plant in Italy. Water 11(8):1599. https://doi.org/10.3390/w11081599

Valentin MM, Hogue TS, Hay LE (2018) Hydrologic regime changes in a high-latitude glacierized watershed under future climate conditions. Water 10(2):128. https://doi.org/10.3390/w10020128

Valt M, Guyennon N, Salerno F, Petrangeli AB, Salvatori R, Cianfarra P, Romano E (2018) Predicting new snow density in the Italian Alps: a variability analysis based on 10 years of measurements. Hydrol Process 32(20):3174–3187. https://doi.org/10.1002/hyp.13249

Wang H, Killick R, Fu X (2014) Distributional change of monthly precipitation due to climate change: comprehensive examination of dataset in southeastern United States. Hydrol Process 28(20):5212–5219. https://doi.org/10.1002/hyp.9999

Webb MJ, Winter JM, Spera SA, Chipman JW, Osterberg EC (2021) Water, agriculture, and climate dynamics in central Chile's Aconcagua River Basin. Phys Geogr 42(5):395–415. https://doi.org/10.1080/02723646.2020.1790719

World Meteorological Organization (2017) Guidelines on the calculation of climate normals (WMO-No. 1203). WMO, Geneva

Zemp M, Paul F, Hoelze M, Haeberli W (2008) Glacier fluctuations in the European Alps, 1850–2000: an overview and spatio-temporal analysis of available data. In: Orlove B, Wiegandt E, Luckman BH, (eds) Darkening Peaks: Glacier Retreat, Science, and Society. University of California Press, Berkeley, CA, pp 152–167